Technical Report 1487
December 1991

Remote Sensing of Trapping Layer Base Height Using ATIS Transmissions

T. M. Vuong

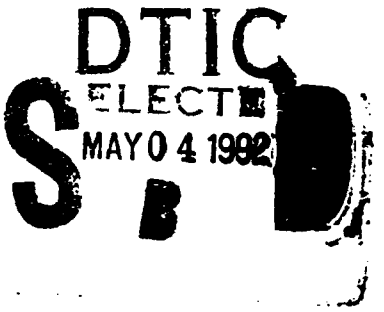

NAVAL OCEAN SYSTEMS CENTER
San Diego, California 92152-5000

J. D. FONTANA, CAPT, USN
Commander

R. T. SHEARER, Acting
Technical Director

ADMINISTRATIVE INFORMATION

This work was performed for the Space and Naval Warfare Systems Command, Washington, DC 20363-5000, by the Naval Ocean Systems Center, San Diego, CA 92152-5000, Ocean and Atmospheric Sciences Division, Code 54.

Released by
R. A. Paulus Head
Tropospheric Branch

Under authority of
J. H. Richter, Head
Ocean and Atmospheric
Sciences Division

LL

CONTENTS

FIGURES

TABLES

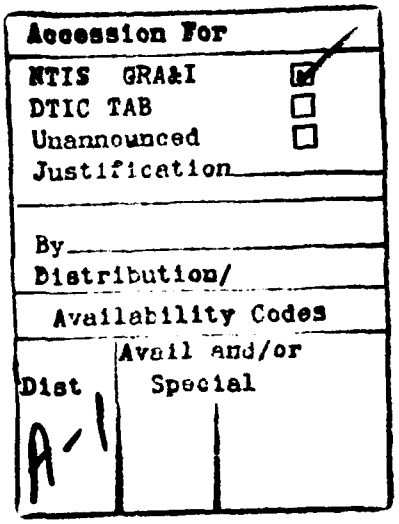

INTRODUCTION

Hitney (1992) presented a method to remotely sense the refractivity structure of the troposphere. This method allows the base of a trapping layer to be determined directly from radio measurements. Since radio signal strength can be computed as a function of the trapping layer base height using the Naval Ocean Systems Center Radio Physical Optics (RPO) model, the observed signal strength may be similarly applied to the RPO model to infer the base height.

This method has been applied to the data of a few UHF signals that were recorded in 1945 during the San Pedro-Point Loma experiment (Hitney, 1992, and Anderson, 1944). The 40-day period of continuous radio data and meteorological measurements shows a remarkable negative correlation between the received signal strengths and the base of the temperature inversion. This suggests the base height of the trapping layer, usually associated with a temperature inversion, is an important factor in influencing radio propagation on over-the-horizon paths. Assuming horizontally homogeneous refractivity conditions and a simple tri-linear modified refractivity profile, the RPO propagation model is applied to the 100-MHz and 547-MHz data sets. Such applications result in inferred base heights that compare quite well to the measured base heights, especially for the higher frequency signal. However, the comparison of a few predictions to the measured data set is not a satisfactory validation of the method, nor a confirmation of its limitations. Therefore, this remote sensing technique requires some further investigations.

INVESTIGATION

An experiment has been conducted to sense signal levels of several VHF and UHF paths along the coast of southern California. The sources of these signals are from Automatic Terminal Information Service (ATIS) broadcasts for airports along the southern California coast (table 1). These ATIS sources are selected such that with the

Table 1. ATIS frequencies in southern California.

MHz	Latitude	Longitude	Airport Name	Elev. (msl)	Distance**
117.20	33°40.3'N	117°43.6'W	El Toro MCAS	117 m	119 km
118.05	34°12.0'N	119°12.3'W	Oxnard	13 m	148 km
119.15	34°00.9'N	118°27.0'W	Santa Monica Mun.	53 m	186 km
120.15	33°07.6'N	117°16.7'W	McClellan-Palomar	100 m	50 km
*125.55	34°07.2'N	119°07.2'W	Point Mugu NAS	4 m	236 km
125.60	33°48.2'N	118°20.3'W	Torrance Mun.	31 m	161 km
126.00	33°40.5'N	117°52.0'W	John Wayne—Orange Co.	16 m	125 km
127.75	33°49.0'N	118°01.0'W	Long Beach; Daugherty	17 m	145 km
127.80	34°25.5'N	119°50.3'W	Santa Barbara Mun.	3 m	308 km
133.80	33°56.5'N	118°24.4'W	Los Angeles Int'l (Arv)	38 m	177 km
*135.65	33°56.5'N	118°24.4'W	Los Angeles Int'l (Dep)	38 m	177 km
267.60	33°18.1'N	117°21.3'W	Camp Pendleton MCAS	24 m	70 km
268.60	33°01.4'N	118°35.2'W	San Clemente Is. NALF	55 m	131 km
277.20	34°07.2'N	119°07.2'W	Point Mugu NAS	4 m	236 km
*284.20	33°40.3'N	117°43.6'W	El Toro MCAS	117 m	119 km
384.30	33°42.4'N	117°49.6'W	Tustin MCAS	16 m	126 km

*Additional frequencies
**Distance from NOSC (32°41'N, 117°15'W).

receiver placed at Point Loma (NOSC Building 323), the transmission paths are well beyond the horizon and mostly over water (figure 1). There are 16 ATIS frequencies of interest which range from 117 MHz to 385 MHz. The transmitters are located from 3- to 177-meters above mean sea-level (msl), and they formed transmission paths from 50- to 300-km in length.

RF DATA ACQUISITION SYSTEM

At NOSC, where the radio measurement is recorded, an LP-1019BA log-periodic antenna was mounted for vertical polarization on the roof of Building 323, at about 40 m above msl, and pointed to the northwest (bearing 320°). From there the received RF signal is fed through a 40-foot RG214 coaxial cable and monitored by an HP-8566B Spectrum Analyzer. The HP-8566B's frequency range and sensitivity are fully adequate for detecting the ATIS signals. For automatic data acquisition, the HP-8566B is connected to an 80286 microcomputer via an IEEE 488 bus. A National Instrument GPIB-II IEEE 488 interface board is used to provide software control of the IEEE bus with the microcomputer.

A simple C-Language program (ATIS.C) was developed to monitor the received ATIS signals and to record the signal levels. The program typically sets the HP-8566B's RF input attenuation at 0 dB, center frequency at an ATIS frequency, the frequency span at 10 kHz, with resolution bandwidth at 100 Hz, and video bandwidth at 300 Hz. The analyzer is also programmed to perform video averaging of five sweeps for each signal, to optimize signal detection. For each ATIS signal, its frequency, signal-to-noise ratio (referenced to 100 Hz bandwidth), and propagation loss are recorded with an effective sample time of 15 seconds. For a one-way transmission system, the propagation loss (in dB) is

$$L = P_t + G_t - P_r + G_r + G_c ,$$

where P_t is the power transmitted, G_t and G_r are transmitter and receiver antenna gains, P_r is the signal power received, and G_c is the coax gain measured from the receiver antenna to the RF input of the analyzer. The typical ATIS antenna is omni-directional and radiates at about 10 watts, making the sum of the first two terms equal to 40 dBm. The high directive gain of the LP-1019BA receiver antenna is about 8 dB, and the cable gain G_c was measured as -1.0 to -2.0 dB. (See table 2.)

In operation, the above measurements are automatically stored on disk files as ASCII text format, for further processing. The measurements are recorded 24 hours per day, at intervals of 15 minutes. The recording began in late September 1991 and is ongoing. However, there are gaps in the data, due to software and hardware failures that were eventually corrected. Table 3 shows the time periods in which measurements were made.

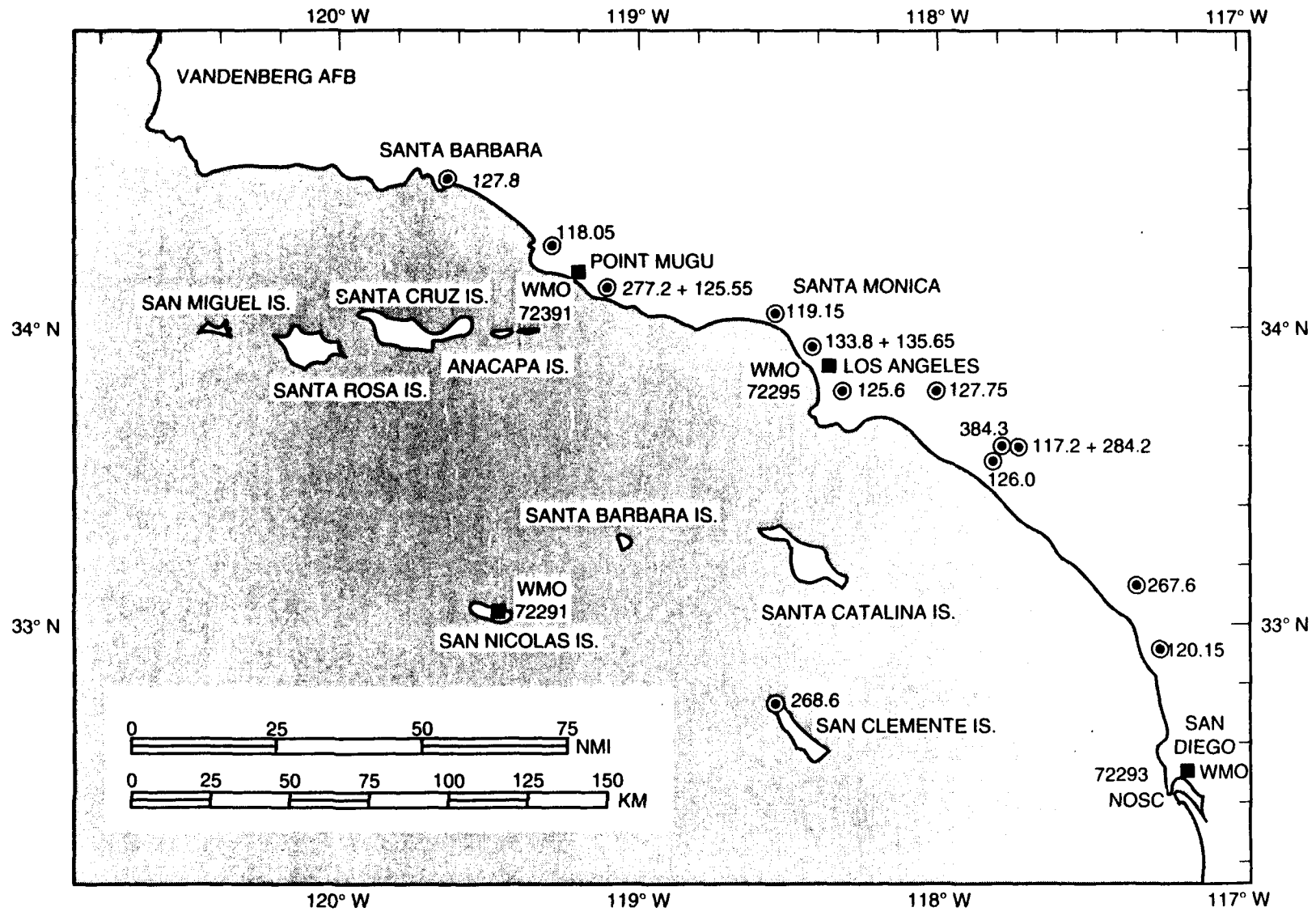

Figure 1. ATIS frequencies and locations.

Table 2. RF system constants.

ATIS Freq (MHz)	Tx Power (dBm)	Coax Gain G_c (dB)
117.20	40.0	-1.00
118.05	40.0	-1.04
119.15	40.0	-1.03
120.15	39.8	-1.03
121.15	40.0	-1.04
125.55	36.0	-1.06
125.60	40.0	-1.06
126.00	40.0	-1.06
127.75	40.0	-1.06
127.80	40.0	-1.06
133.80	40.0	-1.10
267.60	39.0	-1.62
268.60	40.0	-1.62
277.20	36.0	-1.64
284.20	40.0	-1.66
384.30	36.0	-1.99
ATIS transmitter antenna gain (omni)		0 dBi
Receiver antenna gain		8 dB

Table 3. Periods of 1991 ATIS measurements.

Start	End
September 30	October 11
October 23	November 14
November 19	December 9

DATA ANALYSIS

As a first step in analyzing the recorded data, we have written a program (PLTATIS.BAS) to graphically present the time-series of observed ATIS signal-to-noise ratio, propagation loss, propagation factor (relative to free space), and inferred trapping layer base height. Figure 2 shows some results from the November 1991 measurement period, indicating the typical variation in signal strengths (associated with the change in trapping layer base height). Notice there are limits for the observed propagation factors (when signal levels are below the noise level), that will also limit the inferred base heights. Determining the trapping layer base height from radio measurements is quite intricate. First, for each of the ATIS paths, the propagation factor must be computed as a function of trapping-layer base height using the RPO propagation model (RPO program).

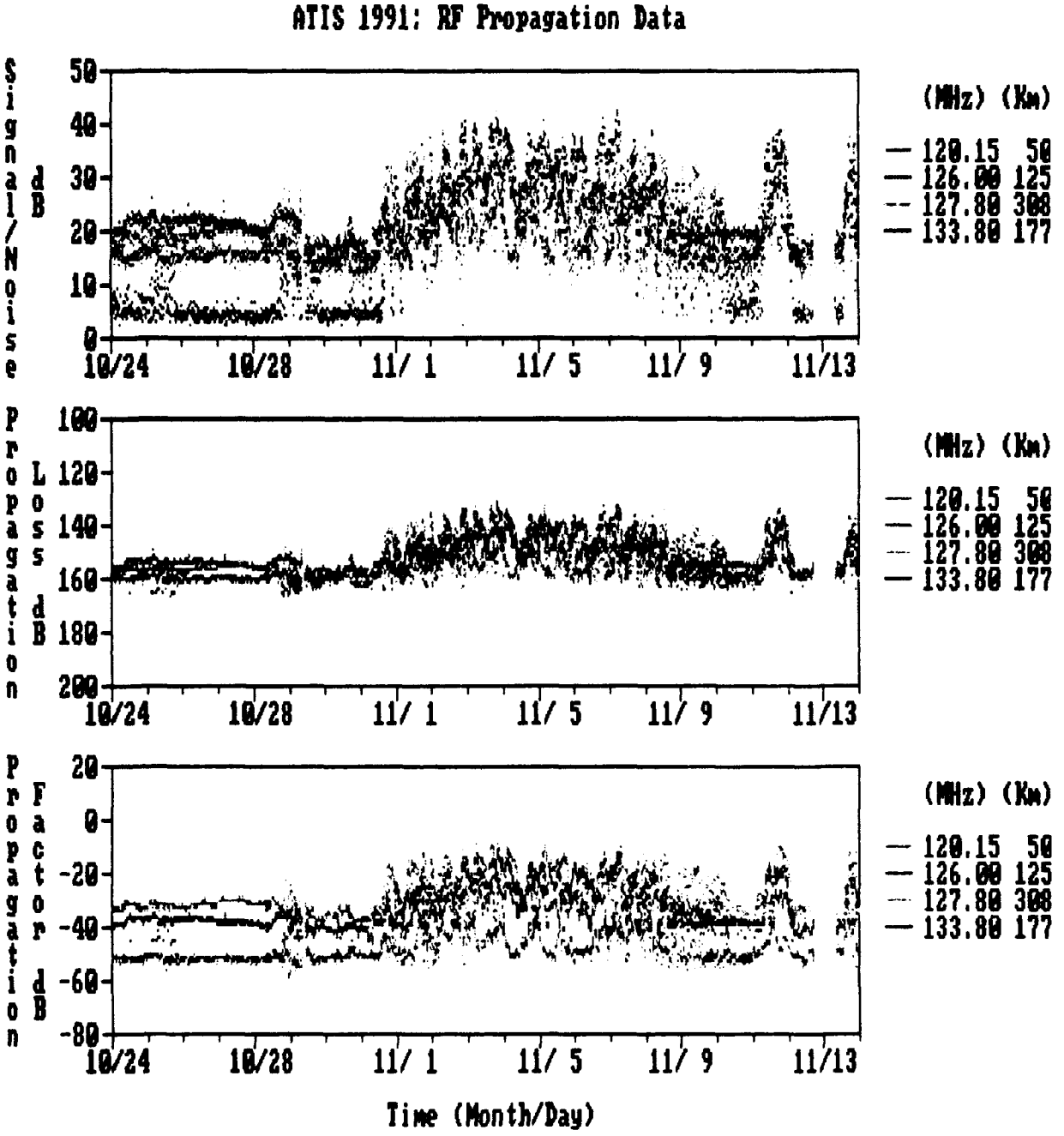

Figure 2. Signal strengths.

Horizontal homogeneity and a simple tri-linear modified refractivity profile, where trapping layer characteristics are derived from historical statistics of the area, are assumed. The tri-linear profile is constructed with a median trapping layer strength of 30 M-units and a thickness of 130 meters. For every value of trapping-layer base heights (0 to 1400 m), the propagation factor calculated by RPO must be read off manually using the EREPS PROPR program. The RPO results for each ATIS frequency are plotted in figures 3a through 3o, and shows propagation factor versus the base of the trapping layer. The line in figures 3a through o is an approximate fit through the first several data points (at base heights lower than 800 m); apparently, there is substantial variation between the data points and especially for the higher trapping layer base heights. The linear regression can be characterized by the slope and the y-intercept of the line. These two quantities are tabulated in table 4 and are used (by PLTATIS.BAS) to compute the inferred base heights from observed propagation factors.

Table 4. Linear approximation of propagation factor versus trapping layer base height for ATIS transmissions.

Frequency (MHz)	Elevation (m)	Range* (km)	Prop. Factor (dB) @0 Bht.	ΔP.F./ΔBht. (dB/m)
117.20	117	119	14.80	-0.078
118.05	13	148	9.00	-0.160
119.15	53	186	5.40	-0.076
120.15	100	50	-0.40	-0.054
125.60	31	161	-1.10	-0.063
126.00	16	125	-5.20	-0.060
127.75	17	145	-4.30	-0.063
127.80	3	308	-0.80	-0.123
133.80	38	177	1.60	-0.068
135.65	38	177	2.10	-0.069
267.80	24	70	6.21	-0.091
268.60	55	131	12.59	-0.065
277.20	4	236	3.40	-0.182
284.20	117	119	12.38	-0.072
384.30	16	126	9.33	-0.072

*Distance from receiver (40 m above msl) at NOSC (32.7°N, 117.25°W)

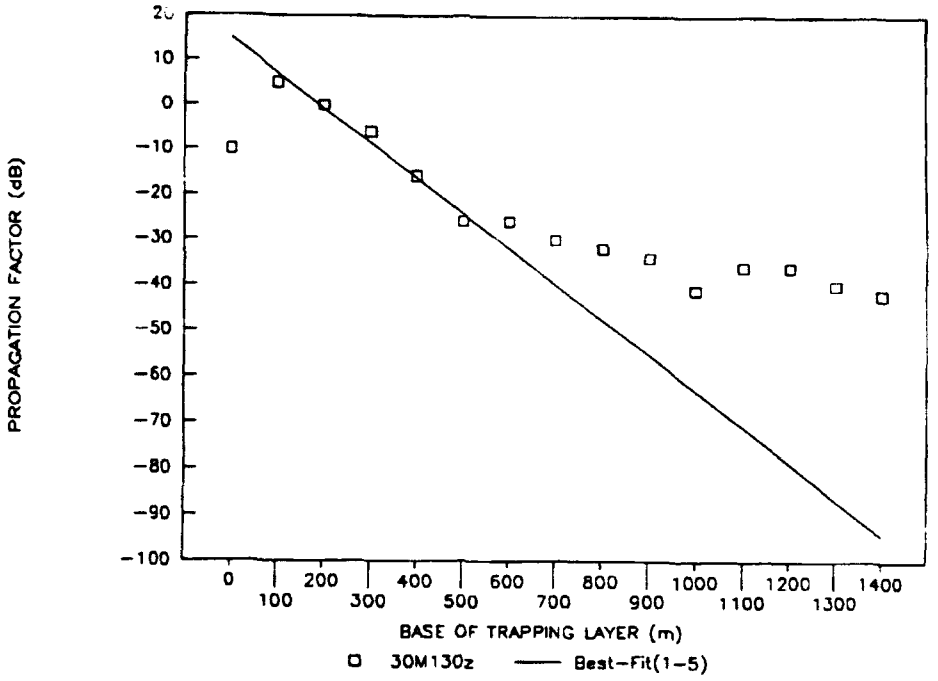

Figure 3a. Propagation factor versus base height at 117.2 MHz (119 km) path.

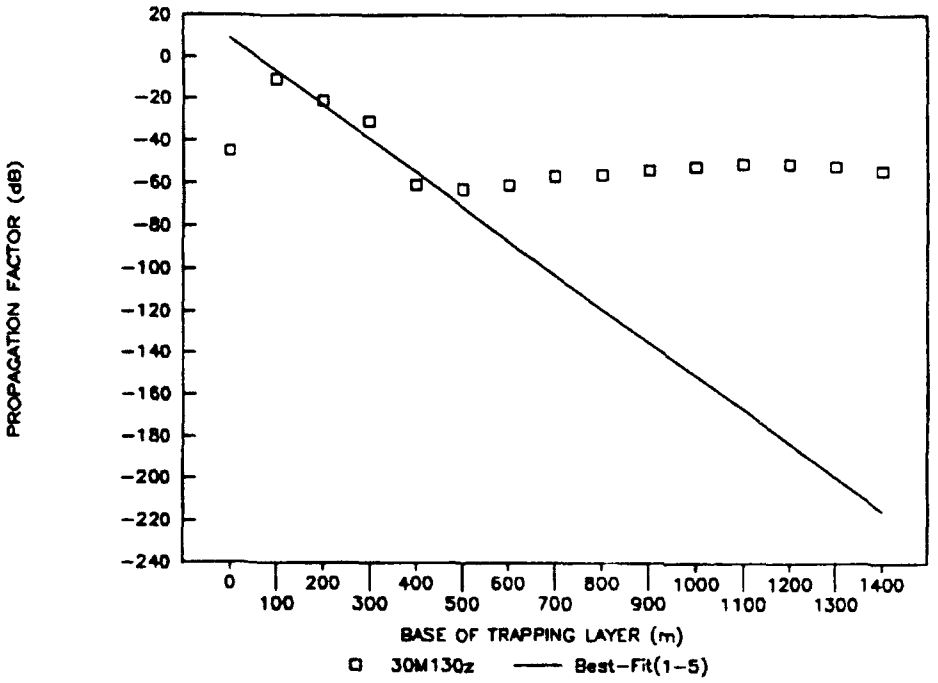

Figure 3b. Propagation factor versus base height at 118.05 MHz (248 km) path.

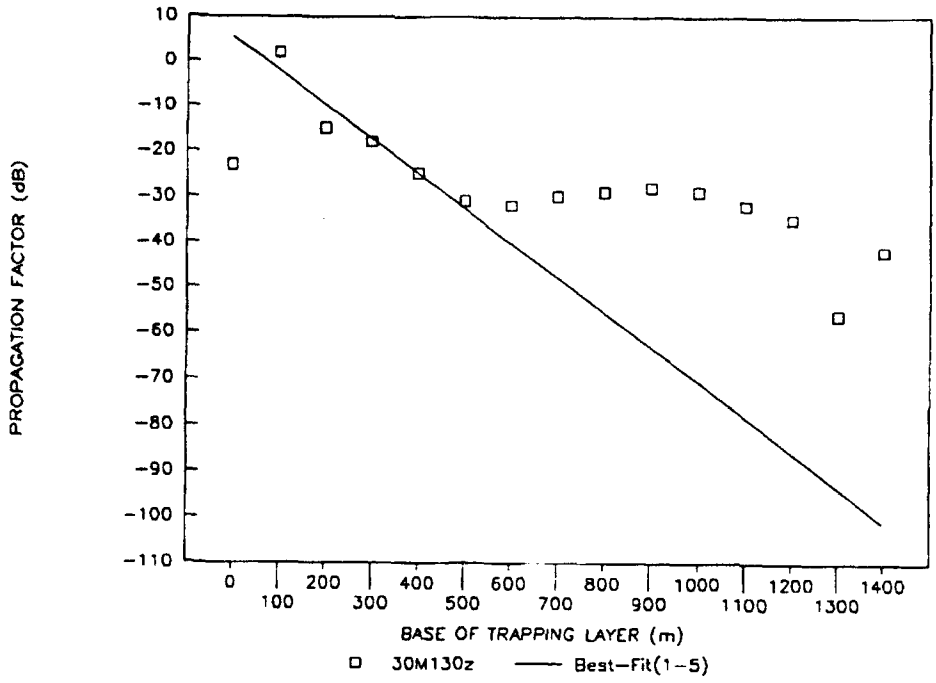

Figure 3c. Propagation factor versus base height at 119.2 MHz (186 km) path.

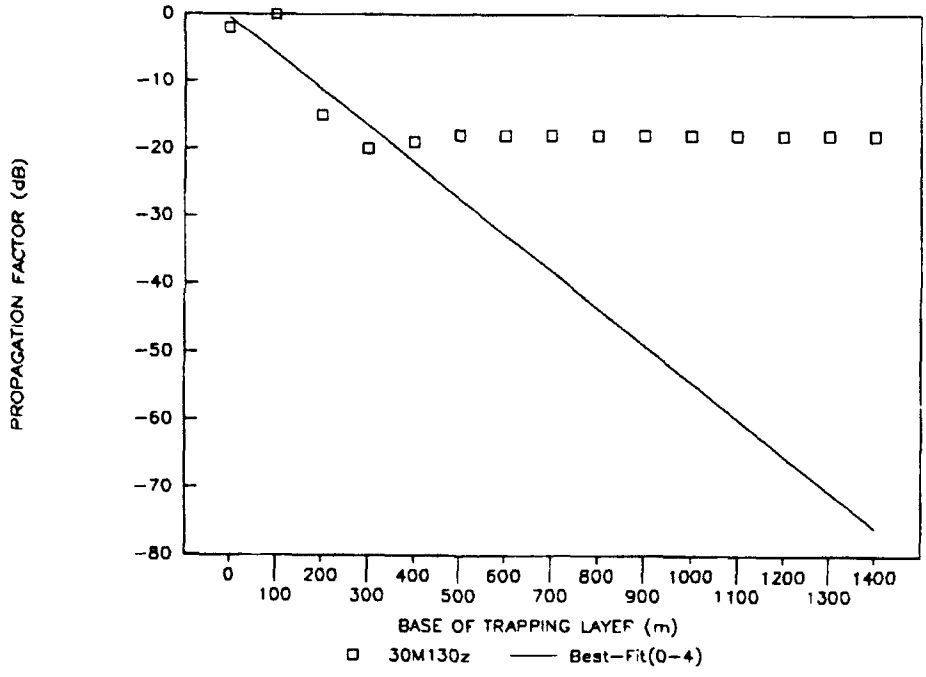

Figure 3d. Propagation factor versus base height at 120.15 MHz (50 km) path.

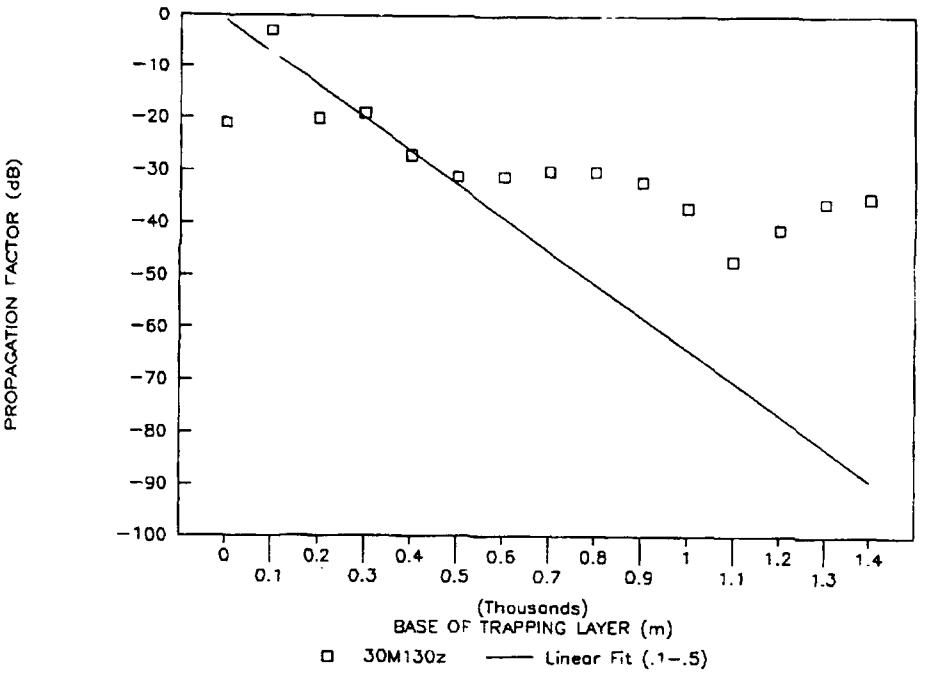

Figure 3e. Propagation factor versus base height at 125.6 MHz (161 km) path.

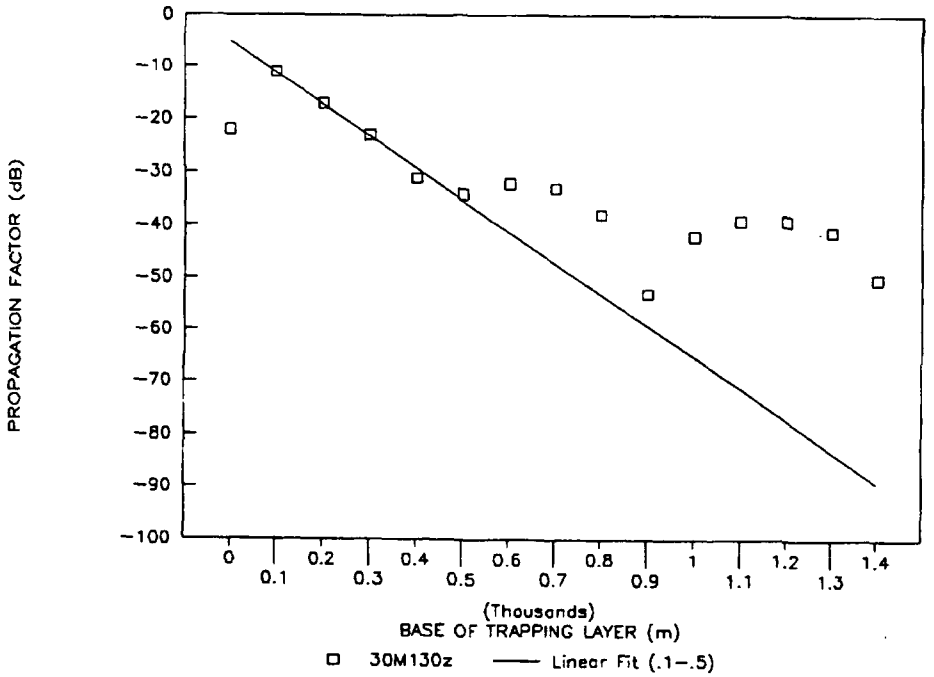

Figure 3f. Propagation factor versus base height at 126 MHz (125 km) path.

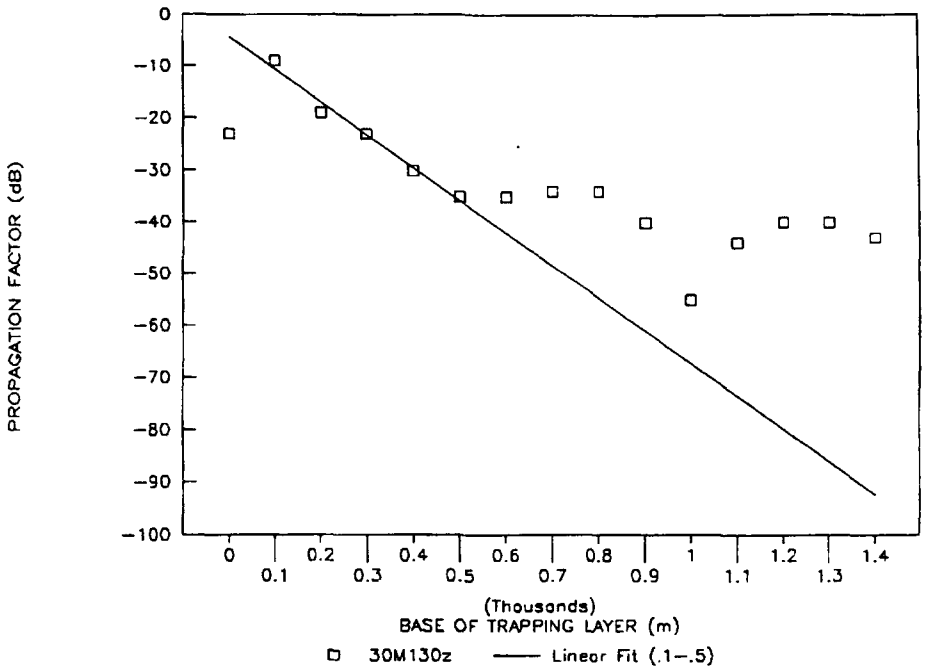

Figure 3g. Propagation factor versus base height at 127.75 MHz (145 km) path.

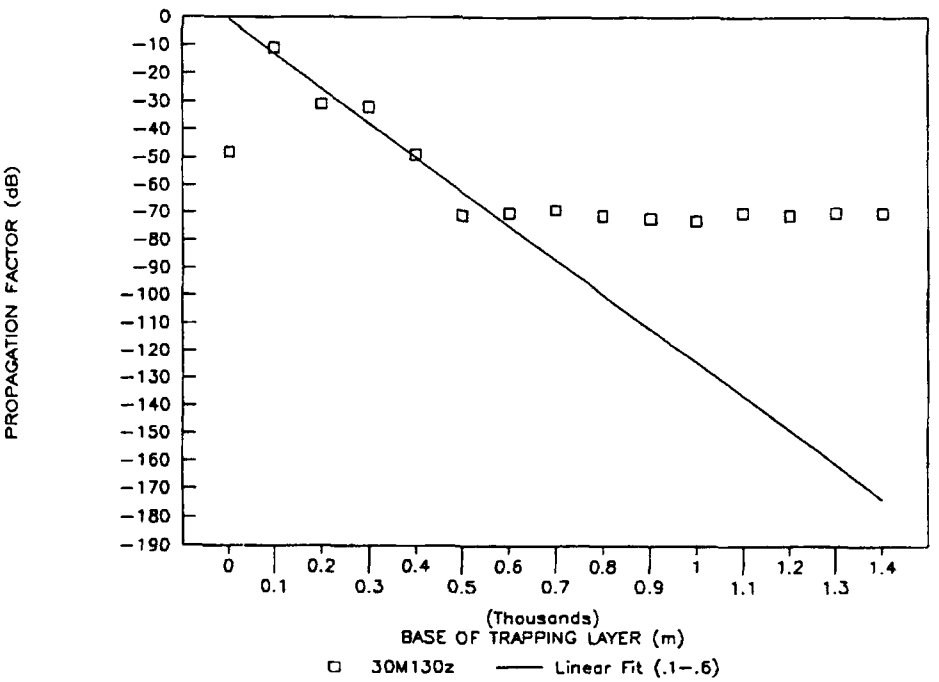

Figure 3h. Propagation factor versus base height at 127.8 MHz (308 km) path.

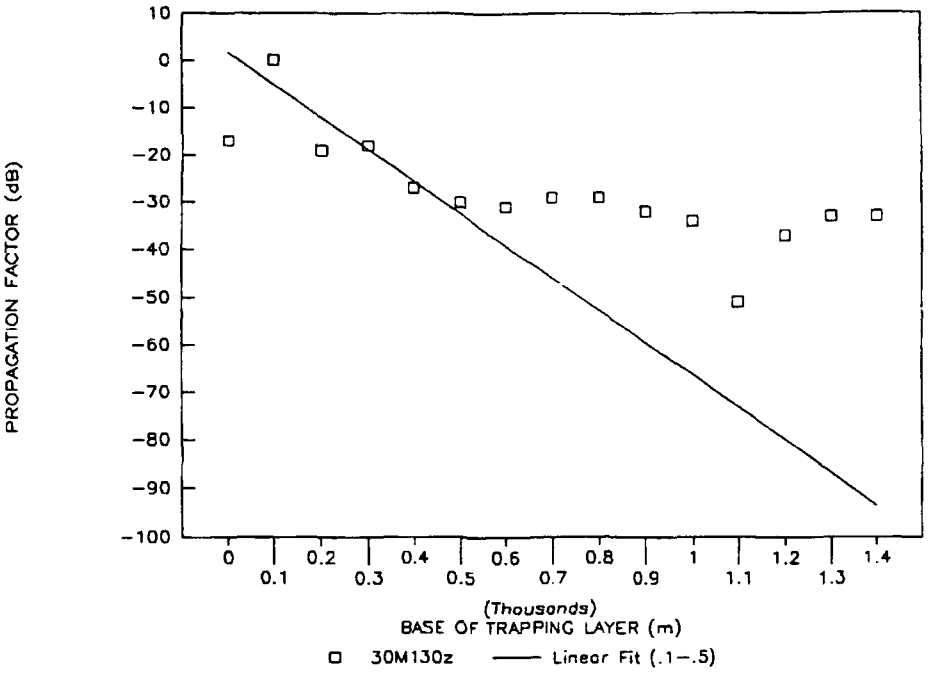

Figure 3i. Propagation factor versus base height at 133.8 MHz (177 km) path.

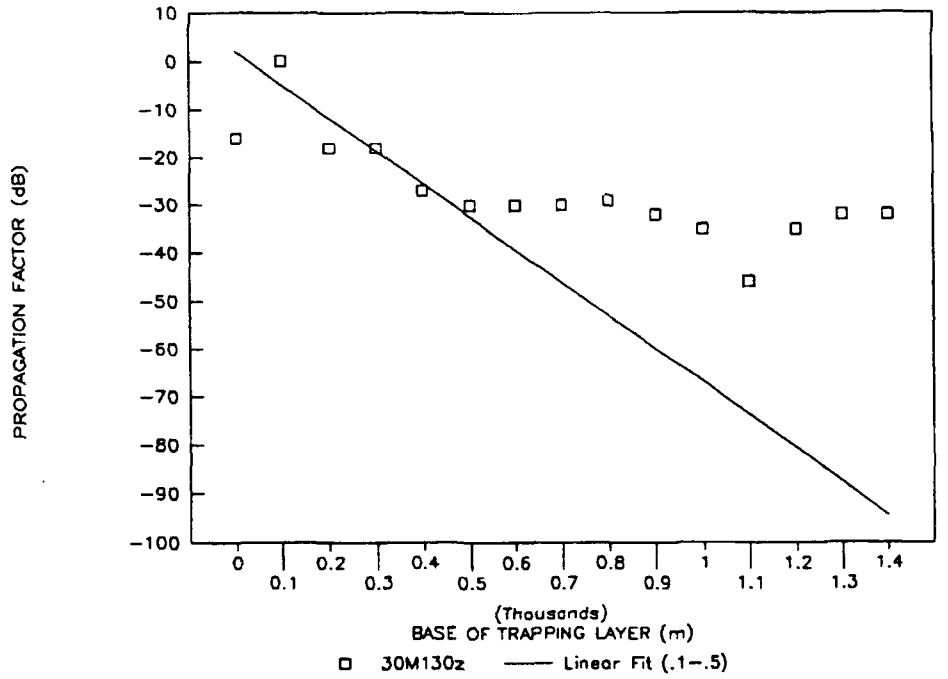

Figure 3j. Propagation factor versus base height at 135.65 MHz (177 km) path.

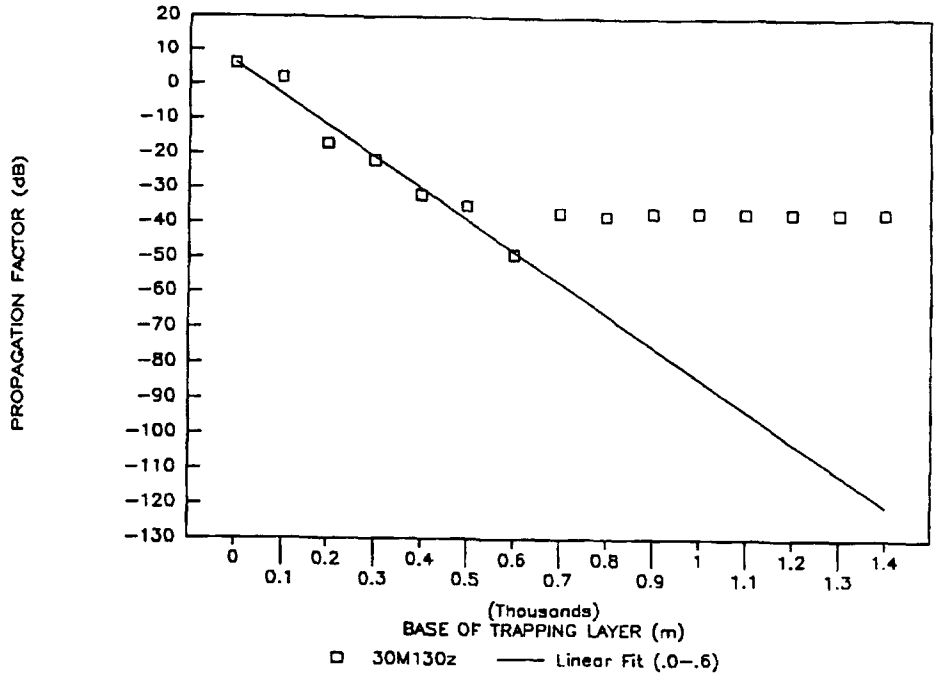

Figure 3k. Propagation factor versus base height at 267.6 MHz (70 km) path.

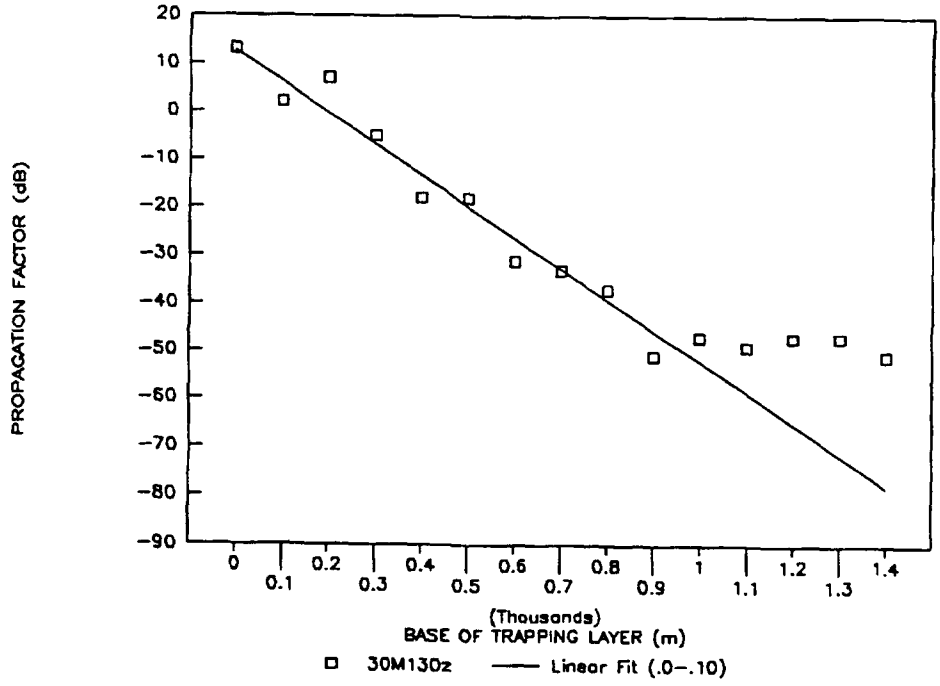

Figure 3l. Propagation factor versus base height at 268.6 MHz (131 km) path.

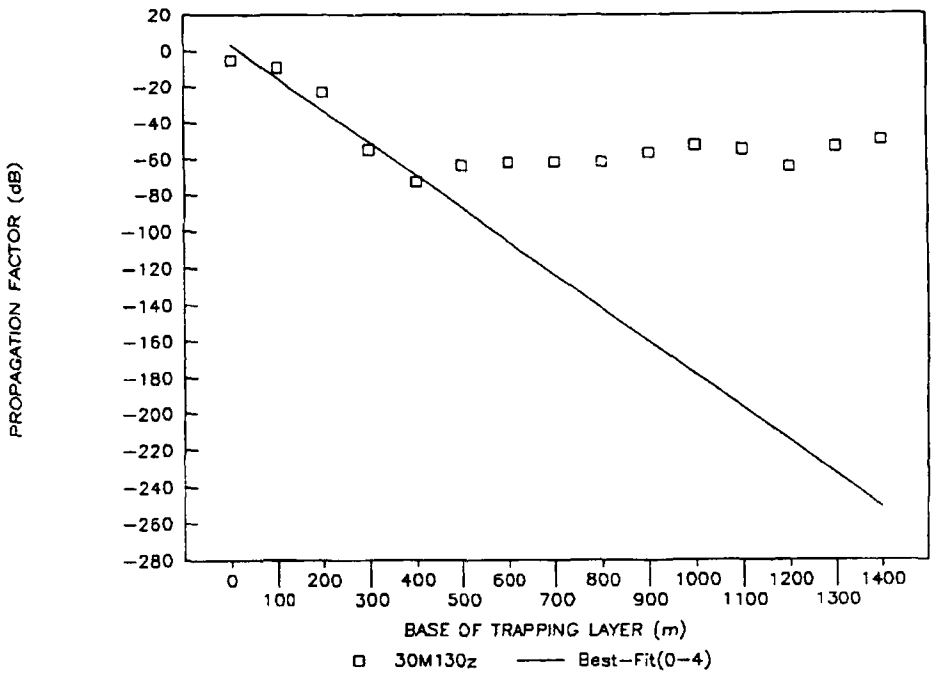

Figure 3m. Propagation factor versus base height at 277.2 MHz (236 km) path.

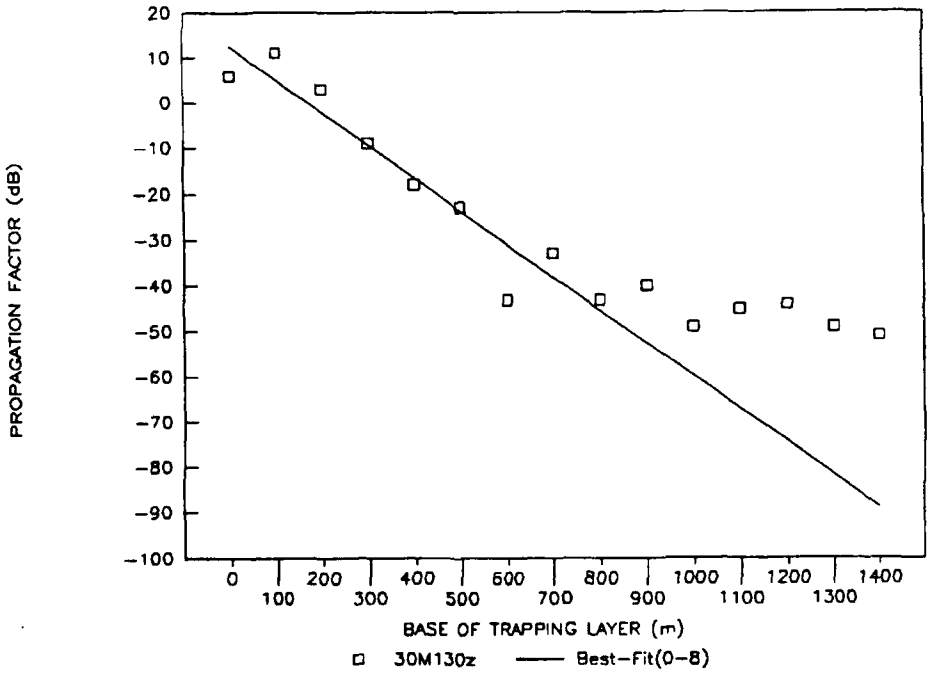

Figure 3n. Propagation factor versus base height at 284.2 MHz (119 km) path.

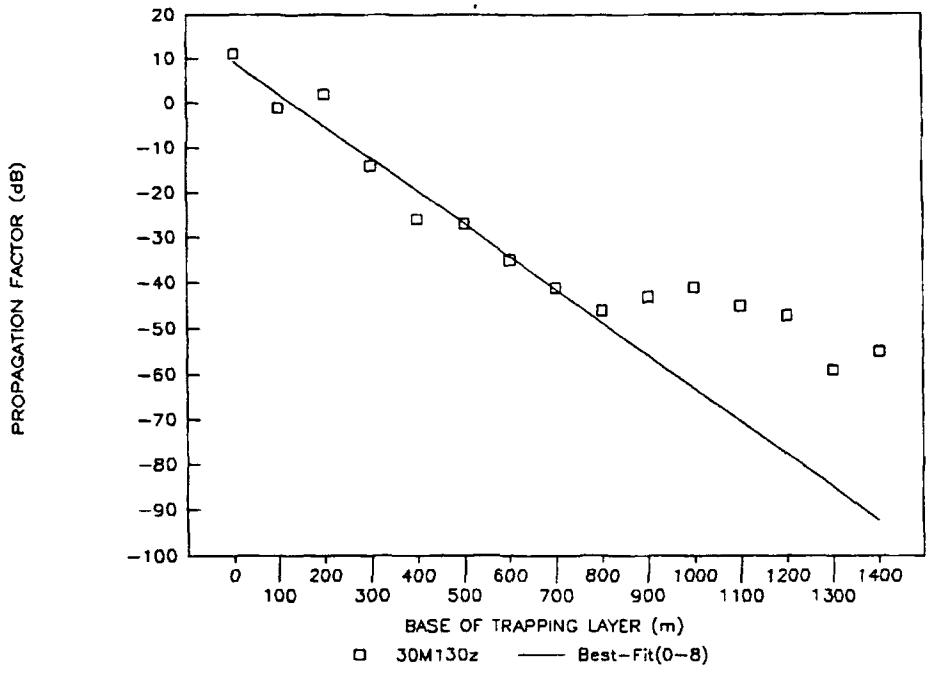

Figure 3o. Propagation factor versus base height at 384.3 MHz (126 km) path.

RESULTS

Typical time-series plots of inferred base heights, figure 4, show good correlation of temporal variation; ATIS sources near each other give almost the same inferred trapping base heights, especially in the Los Angeles area. However, the inferred base heights also vary extensively for some of the other paths. Such disagreement is perhaps a result of the uncertainty in linear regression of the computed propagation factors versus trapping base heights, because there are substantial deviation errors in the linear approximation. Furthermore, as shown in scatter plots of figure 5, observed trapping base heights generally do not agree with the base heights inferred from the radio data, nor do they agree with each other. This is probably an indication that the assumption of horizontal homogeniety does not always hold.

In any case, additional measured data of base heights are required to verify the extent of any nonhomogeneous condition and to explain the discrepancies between prediction and observation of trapping layer base heights. Thus far in this experiment, the measured data available are from the radiosonde observations of a few World Meteorological Organization (WMO) stations in southern California. Since most of these stations are located away from the transmission paths of interest and their radiosonde observations are sporadically reported, the available data are not reliable or useful.

CONCLUSIONS

A remote sensing experiment has been established to examine the method of determining base heights of a trapping layer directly from VHF and UHF radio measurements. The setup of this experiment is relatively simple and convenient; it uses existing radio broadcasts along the coast of southern California as sources of signal propagation and requires minimal equipment to record the signal strengths of such transmissions.

However, the technique of processing the recorded data to infer trapping layer base heights is somewhat uncertain. The linear formulation of propagation factor as a function of base height from the RPO propagation model is only an approximation; hence, errors are expected in the inferred base heights. In addition, considerations of horizontal homogeneity may be invalid. Further investigation into these problems may provide improvement for the technique. Nevertheless, the experiment shows some strong correlations between the observed signal strengths as well as the inferred trapping layer base heights of the various radio paths, indicating the height of the trapping layer is an important factor in controlling radio propagation on over-the-horizon paths.

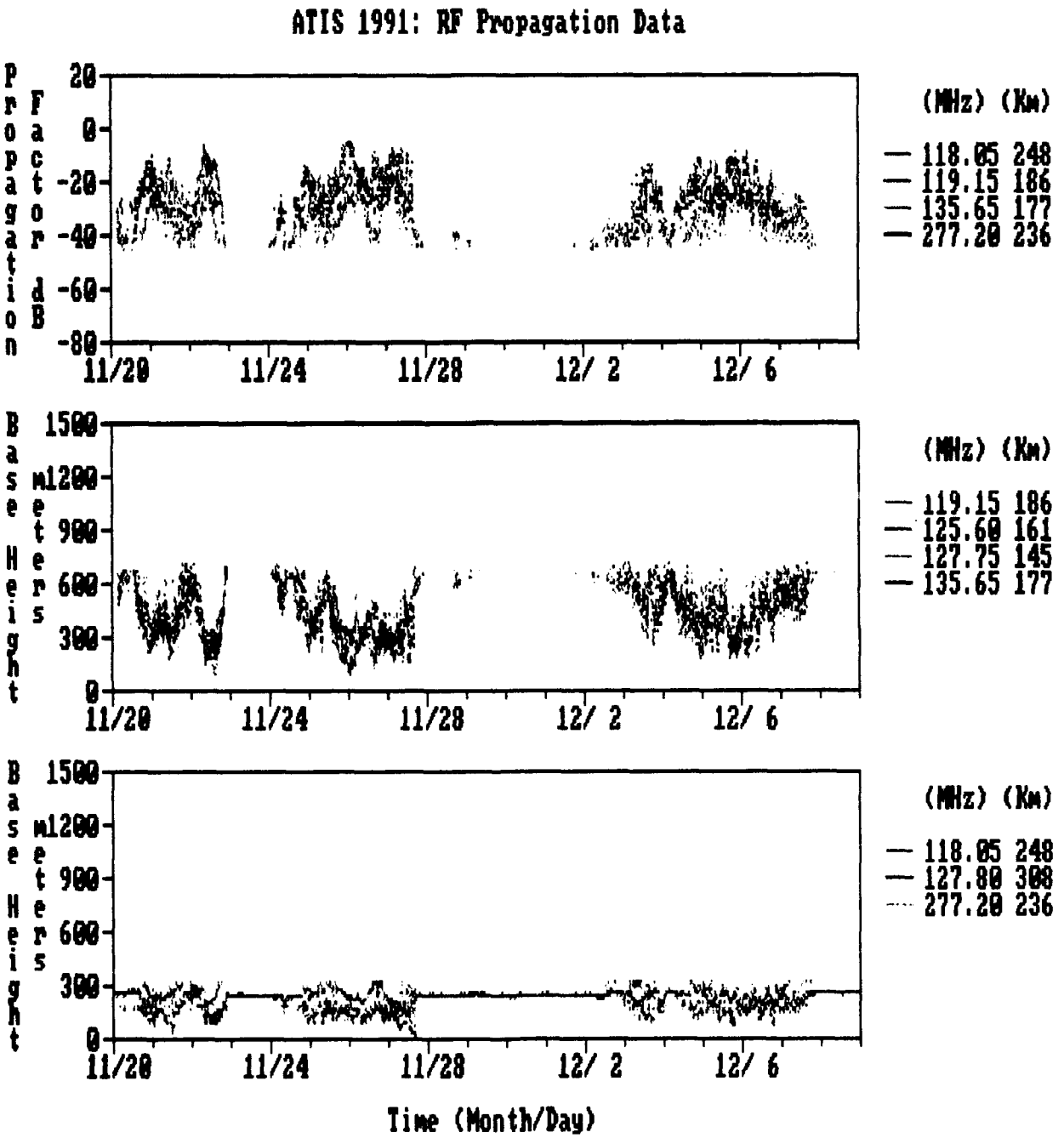

Figure 4. Inferred trapping layer base heights.

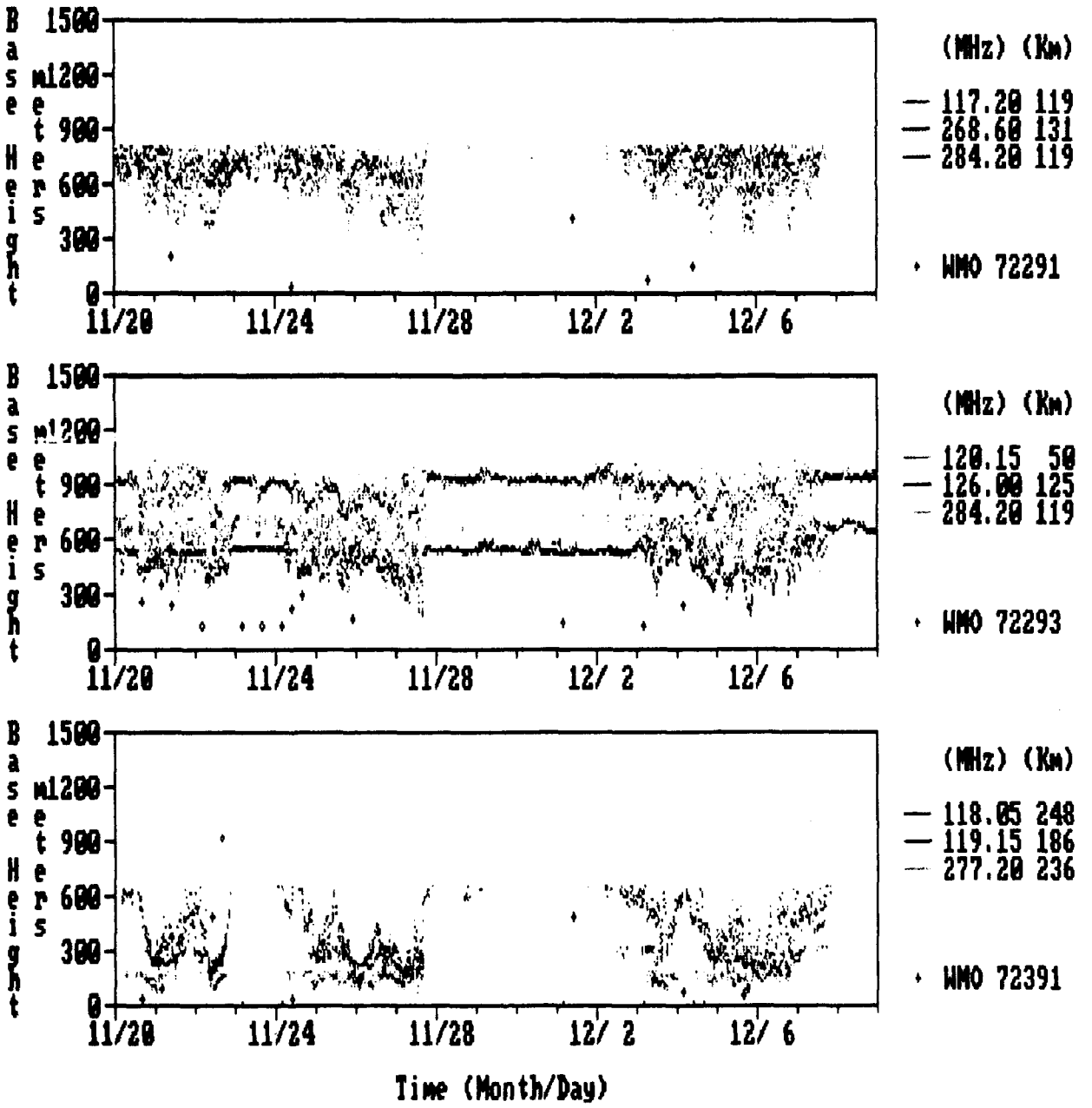

Figure 5. Observed and inferred base of trapping layer.

REFERENCES

Anderson, L. J. 1944. "Atmosphere Refraction—A Preliminary Quantitative Investigation," NRSL Report No. WP-17.

Hitney, H. V. 1992. "Remote Sensing of Refractivity Structure by Direct Radio Measurements at UHF," in *Remote Sensing of the Propagation Environment*, CP 502, pp. 1.1-1.5.

REPORT DOCUMENTATION PAGE

Form Approved
OMB No. 0704-0188

1. AGENCY USE ONLY *(Leave blank)*	2. REPORT DATE	3. REPORT TYPE AND DATES COVERED
	December 1991	Final

4. TITLE AND SUBTITLE

REMOTE SENSING OF TRAPPING LAYER BASE HEIGHT USING ATIS TRANSMISSIONS

5. FUNDING NUMBERS

PE: 0602435N
PROJ: RM35
WU: DN488760

6. AUTHOR(S)

T. M. Vuong

7. PERFORMING ORGANIZATION NAME(S) AND ADDRESS(ES)

Naval Ocean Systems Center
San Diego, CA 92152–5000

8. PERFORMING ORGANIZATION REPORT NUMBER

NOSC TR 1487

9. SPONSORING/MONITORING AGENCY NAME(S) AND ADDRESS(ES)

Space and Naval Warfare Systems Command
Washington, DC 20363–5000

10. SPONSORING/MONITORING AGENCY REPORT NUMBER

11. SUPPLEMENTARY NOTES

12a. DISTRIBUTION/AVAILABILITY STATEMENT

Approved for public release; distribution is unlimited

12b. DISTRIBUTION CODE

13. ABSTRACT *(Maximum 200 words)*

This report describes an experiment that examined the method of determining base heights of a trapping layer directly from VHF and UHF radio measurements. The experiment used existing radio broadcasts along the coast of southern California. Some strong correlations between the observed signal strengths and the inferred trapping layer base heights of the various radio paths were shown, indicating the height of the trapping layer is an important factor in controlling radio propagation on over-the-horizon paths.

14. SUBJECT TERMS

trapping layer
radio propagation
ATIS transmissions
remote sensing
horizontal homogeneity
refractivity

15. NUMBER OF PAGES

26

16. PRICE CODE

17. SECURITY CLASSIFICATION OF REPORT	18. SECURITY CLASSIFICATION OF THIS PAGE	19. SECURITY CLASSIFICATION OF ABSTRACT	20. LIMITATION OF ABSTRACT
UNCLASSIFIED	UNCLASSIFIED	UNCLASSIFIED	SAME AS REPORT

21a. NAME OF RESPONSIBLE INDIVIDUAL	21b. TELEPHONE *(include Area Code)*	21c. OFFICE SYMBOL
T. M. Vuong	(619) 553-1424	Code 543

INITIAL DISTRIBUTION

Code 0012	Patent Counsel	(1)
Code 0144	R. November	(1)
Code 50	H. O. Porter	(1)
Code 54	J. H. Richter	(1)
Code 543	R. Paulus	(20)
Code 952B	J. Puleo	(1)
Code 961	Archive/Stock	(6)
Code 964B	Library	(3)

Defense Technical Information Center
Alexandria, VA 22304-6145 (4)

NCCOSC Washington Liaison Office
Washington, DC 20363-5100

Center for Naval Analyses
Alexandria, VA 22302-0268

Navy Acquisition, Research & Development
Information Center (NARDIC)
Alexandria, VA 22333

Navy Acquisition, Research & Development
Information Center (NARDIC)
Pasadena, CA 91106-3955

Office of Naval Technology
Arlington, VA 22217-5000 (2)

Pacific Missile Test Center
Point Mugu, CA 93042-5000 (2)

Naval Oceanographic & Atmospheric (2)
Research Laboratory
Stennis Space Center, MS 39529-5004